

Article

Building–Soil Thermal Interaction: A Case Study

Grzegorz Nawalany * and Paweł Sokołowski

Department of Rural Building, Faculty of Environmental Engineering, University of Agriculture in Krakow, 30-059 Krakow, Poland

* Correspondence: grzegorz.nawalany@urk.edu.pl; Tel.: +48-12-662-4009

Received: 5 June 2019; Accepted: 27 July 2019; Published: 29 July 2019



Abstract: This paper presents an analysis of thermal interaction between a building and surrounding soil. The examined building was located in southern Poland. Measurements of selected indoor and outdoor air temperature parameters were made in order to determine the boundary conditions. The soil temperature measurements were conducted at 42 points. The analysis of results is divided into four periods: summer, autumn, winter, and spring. The analysis shows that weather conditions significantly affect the temperature in soil, but the range of residential building impact decreases with distance, and it varies depending on the season. The residential building impact on the soil temperature is in the range of 1.2–3.3 m. This paper also includes a study of the heat flow direction in soil and a quantitative estimate of heat exchange between a building and the soil. The greatest energy losses 2082 kWh (21.24 kWh/m²) from the building to the soil were recorded in winter. In spring, the energy losses were reduced by about 38% as compared with the energy losses in winter, and the energy losses in spring were comparable to autumn.

Keywords: heat exchange with soil; soil temperature; housing; heat accumulation

1. Introduction

The impact of various factors on the environment, over the last few years, has become a major issue. One of the factors that affect the world surrounding us is housing. A dynamic development of construction materials and housing technology improvement has made the buildings significantly more energy efficient [1–3]. A number of standards and legal provisions that determine requirements regarding efficiency and energy consumption of buildings have been created taking into consideration innovative technical solutions. The need to reduce energy has justified using facilities plunged into soil. Soil thermal accumulation and high soil thermal inertia may stabilize internal air temperature and the temperature of compartments that directly touch soil [4–7]. Within the field of energy development, the use of unconventional energy sources has also changed. During the last decade, the use of renewable energy has grown from 250% to as high as 450%, depending on the world region [7].

The temperature variation amplitude in a non-built-up area depends mainly on the air temperature, and also on the land cover, inclination, and exposure. The impact of these factors is strongly noticeable in underground buildings. These types of buildings potentially reduce energy demand, in comparison to conventional above ground buildings, by exploiting the advantage of soil temperatures and ground cover as insulation [8]. The surface soil layer has the greatest temperature variation amplitude, and at the depth of about 10 meters the soil temperature is roughly equal to the average air temperature in a given area [9]. The soil temperature distributions in the vicinity of heated buildings are more complex because they are affected by an additional factor which is the heat stream from the building. The heat exchange between the building and the surrounding soil has some contribution to the building energy balance. This issue is also addressed in numerous calculation-based studies. Numerical methods help to understand the phenomenon of heat exchange from the ground to hypothetical buildings [10–12].

The detailed estimation of heat gains and losses caused by the heat interactions between the building and the soil is a complex task. The heat exchange with soil is a three-dimensional and non-stationary phenomenon [13]. Large phase delays, which are caused by the high heat capacity of soil and temperature variation depending on the conditions at the surface, are the basic factors affecting the complexity of the analysis. Contemporary standard methods [9] are based on a quasi-stationary method developed by Hagentoft in the 1980s which requires many simplifications that make it impossible to determine the heat exchange streams between the building and the soil at every moment.

The subject of heat exchange in soil has been studied, *inter alia*, by Radoń et al. [14], Nawalany et al. [15,16], Staniec [17], Martin and Canas [18], Janssen [19], Deru [20], Popiel and Wojtkowiak [21], Larwa and Kupiec [22], and Staszczuk et al. [23]. In recent years, the issue of soil temperature has been very important to the design of heat pumps and soil heat exchangers which is also reflected in numerous studies [24–29]. Depending on the purpose of a building, the surrounding soil can be a heat receiver or a heat source. Winter is particularly important because the cooled soil in the surroundings of a building increases the heat exchange and the energy demand of the building. Regardless of the heat gains and losses from soil, the range of interactions of these processes is spatially limited [30].

The objective of the paper is to analyze the soil temperatures in the surroundings of a residential building. The results of the study can be used to determine the thermal changes in soil and the soils response to the ambient temperature changes of seasons.

2. Materials and Methods

The subject of the study was a residential building in southern Poland. It was a masonry, single-storey building with a usable attic, on a 60 cm wide continuous footing, 24 cm thick reinforced-concrete foundation walls cast in situ using C16/20 concrete, and 36 cm thick insulated solid outside walls with a heat transfer resistance of $R = 3.35 \text{ W}\cdot\text{m}^{-2}\cdot\text{K}^{-1}$. The roofing was made of cement tiles.

The macroscopic examination of soil showed a 2.5 m thick clay layer under a 0.2 m humus layer. The groundwater table was 6 meters below the ground level.

The soil temperature measurements were conducted in 42 points (Figure 1) using PT100 sensors (0.1°C measuring resolution). The indoor (Θ_i) and outdoor (Θ_e) temperature and relative humidity measurements were made using portable Voltcraft loggers (0.1°C ; 1% measuring resolution).

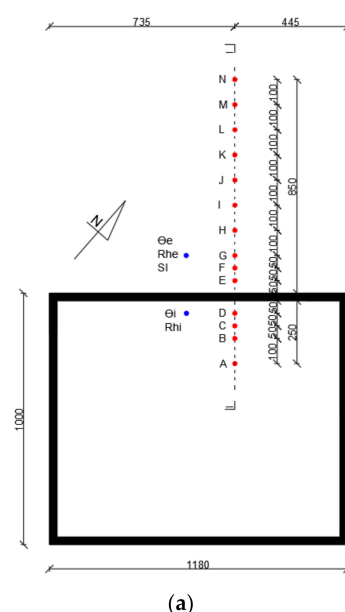


Figure 1. Cont.

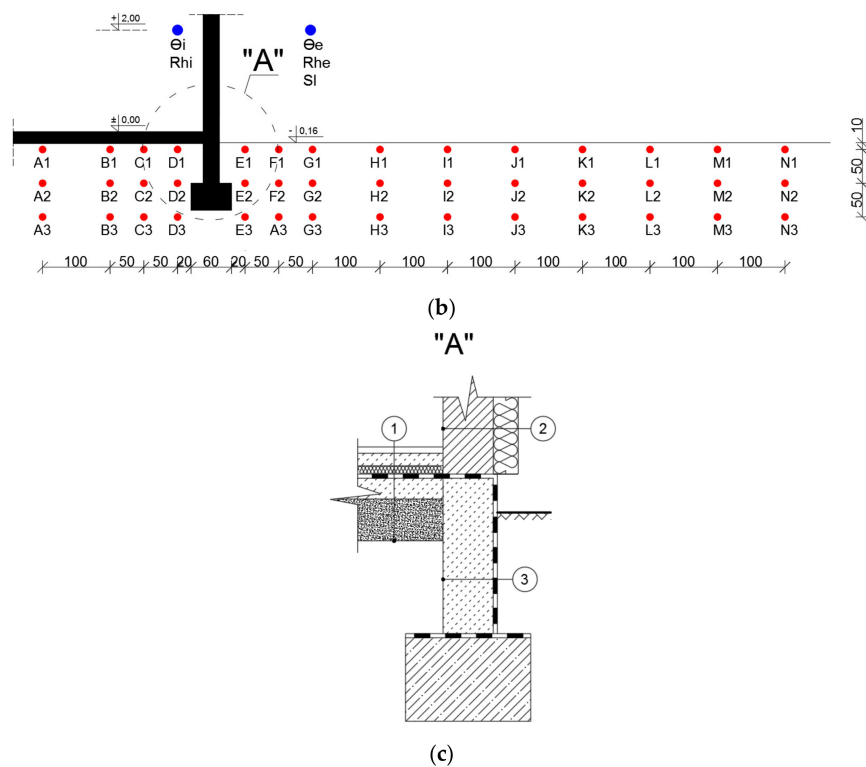


Figure 1. Placement of A1–N3 soil temperature sensors and indoor (Θ_i) and outdoor (Θ_e) air temperature sensors. (a) horizontal projection, (b) cross section I-I, and (c) details of foundation: 1—parquet floor 0.03 m, 2—concrete floor 0.06 m, olyethyl 0.04 m, concrete 0.10 m, sand 0.30 m; 2—breeze blocks 0.24 m, olyethyl 0.12 m, plaster; and 3—concrete blocks 0.24 m, olyethylene mebrane.

The solar irradiance measurements were performed with the LB-901 Kipp&Zonen CMP3 pyranometer. The data sampling interval was 60 min. The studies were conducted between 1 June 2017 and 31 May 2018.

The results of the study were divided into 4 periods: summer (1 June 2017–31 August 2017), autumn (1 September 2017–30 November 2017), winter (1 December 2017–28 February 2018), and spring (1 March 2018–31 May 2018).

The heat exchange with soil was calculated based on the soil temperature 10 cm below the floor and the indoor air temperature using the following equation:

$$q = \frac{\Theta_i - \Theta_g}{\left(\frac{0.1}{\lambda_s}\right) + R_{si}} \left[\text{W} \cdot \text{m}^{-2} \right] \quad (1)$$

In Equation (1), Θ_i is the indoor air temperature, [K], Θ_g if the soil temperature interpolated linearly between points (A1–D1), [K], λ_s is the soil thermal conductivity coefficient assumed at 1.9 W/mK, [EN ISO 6946], R_{si} is the thermal resistance coefficient assumed at 0.14 m²K/W, and 0.1 is the soil temperature 10 cm below the floor.

The data distribution normality was verified using the Shapiro–Wilk test. The results showed that the soil temperature data did not have a normal distribution. Consequently, further statistical analysis was based on a nonparametric Kruskal–Wallis test at the $\alpha = 0.05$ significance level.

3. Results

The studies showed that the indoor temperature was in the range of 19.2–25.9 °C, and the outdoor temperature was in the range of −20.4–30.1 °C. The average annual value of solar radiation was 200.0

W/m². The average value of the relative humidity of the internal air was 60.6%, whereas, the average value of the relative humidity of the external air was 74.0% (Figure 2).

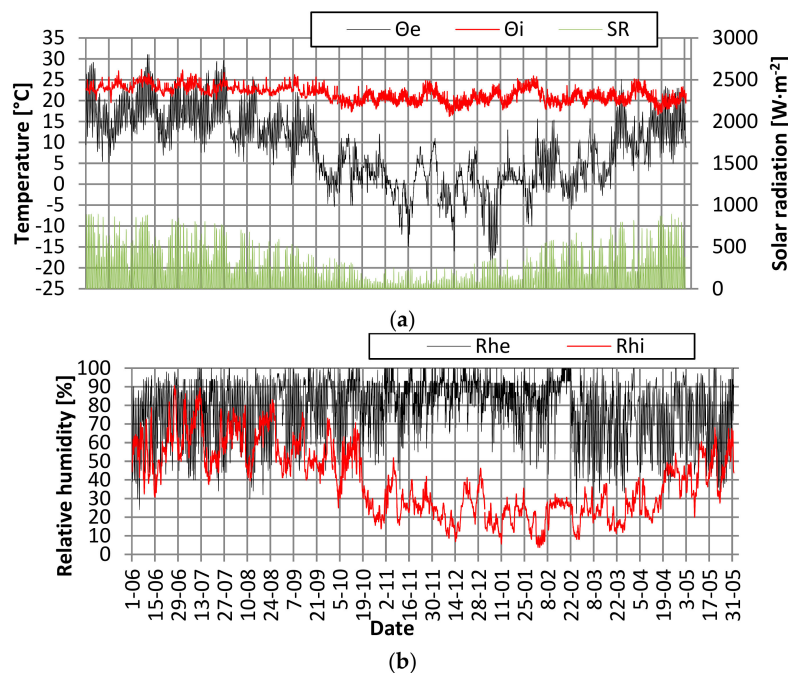


Figure 2. Temperature (a) and relative humidity (b) of interior and exterior air: SR—solar radiation, Θ_e —exterior air temperature, Θ_i —interior air temperature, Rh_e —exterior air relative humidity, and Rh_i —interior air relative humidity.

3.1. Summer Season

Figures 3–6 present the selected soil temperature curves. The soil temperature under the building (lines A–D) was in the range of 16.5–20 °C. The temperatures in the soil surrounding the building (lines E–N) were significantly lower, ranging from 15.6 °C to 17.4 °C near the foundation. The soil temperature dropped to 13.6–17.1 °C as the distance from the building increased. The studies during the summer did not indicate a clear impact of the building on the surrounding soil.

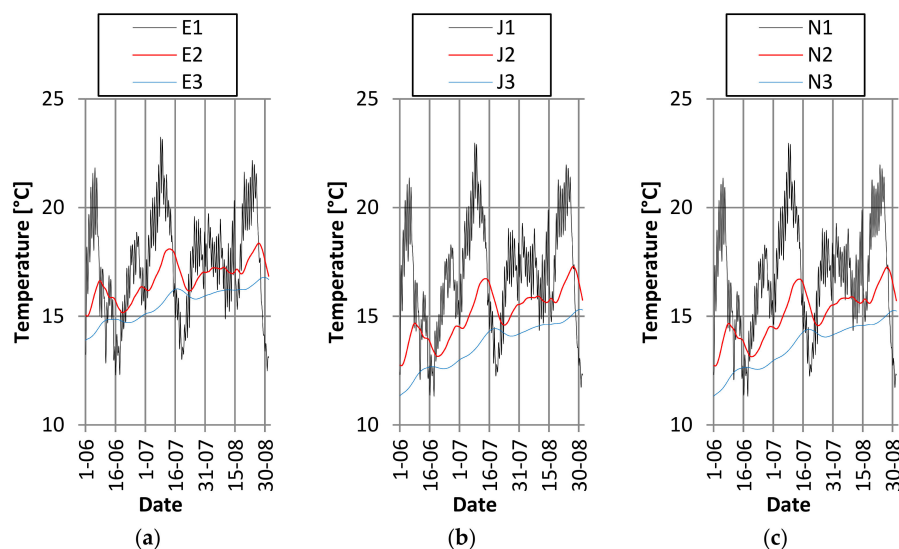


Figure 3. Soil temperature in lines E, J, and N on selected days during the summer season.

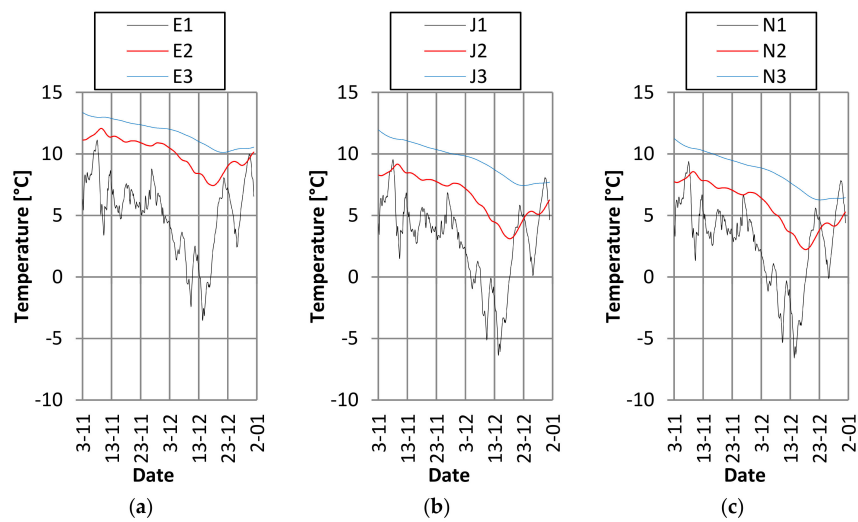


Figure 4. Soil temperature in lines E, J, and N on selected days during the autumn season.

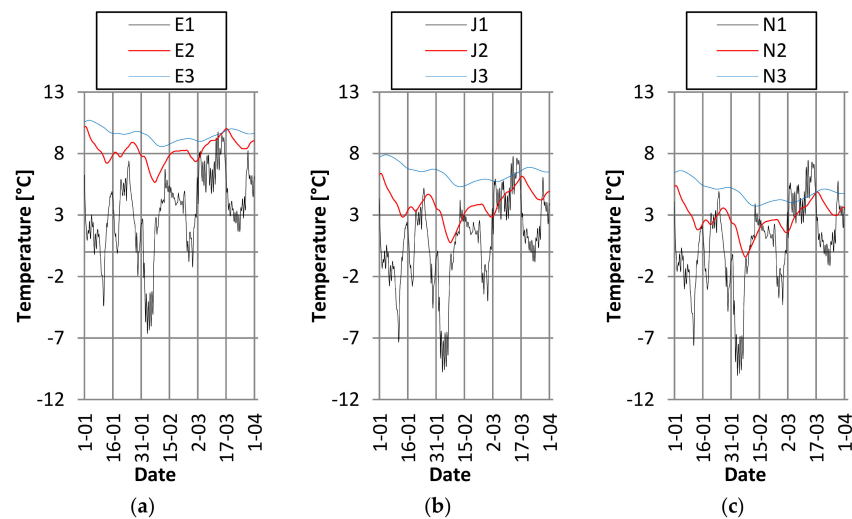


Figure 5. Soil temperature in lines E, J, and N on selected days during the winter season.

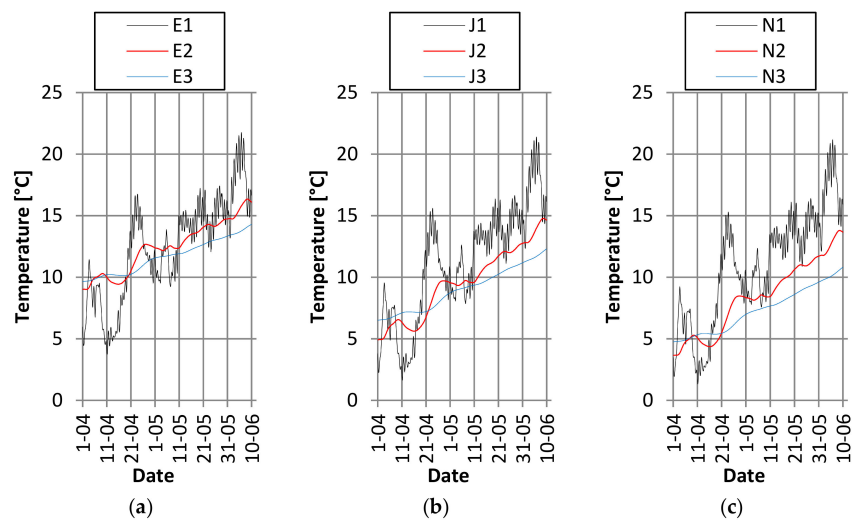


Figure 6. Soil temperature in lines E, J, and N on selected days during the spring season.

3.2. Autumn Season

During the autumn season (Figure 4), the building was constantly heated. The average temperature in November in line E for all depths was 2.5–3 °C higher than the temperature in the same line at the end of the winter period. A temperature difference was also recorded between the line located nearest to the foundation (E) and the farthest to the foundation (N); this difference was 1.7–2.0 °C. The outdoor temperature gradually dropped in November and December, and the soil responded. The first level, located at the depth of 0.10 m, showed a temperature drop of 3.3–3.5 °C, depending on the distance to the building. At the deepest level (1.00 m), the temperature drop was 2.2–2.7 °C. The average temperature difference between the extreme depth levels was 3.1–4.4 °C in November and 4.1–5.2 °C in December.

3.3. Winter Season

The average temperature in January in line E for all depth levels was 3.6–8.5 °C. The temperature increased by about 3.0 °C, (7.8–8.3 °C) in early March. A temperature difference was also recorded between the line located nearest to the foundation (E) and the farthest to the foundation (N). This difference was on average 1.7–2.3 °C (January), 2.9–4.4 °C (February), and 3.6–3.8 °C at the end of winter during the first days of March. The temperatures at the levels of the study gradually dropped during the winter period (Figure 5).

3.4. Spring Season

The temperature range in April in line E for all depth levels was 5.5–16.0 °C. The temperature fluctuated during that period, dropping and rising alternately, however, it slowly increased as the air grew warmer. A temperature difference was also recorded between the line located nearest to the foundation (E) and the farthest to the foundation (N); this difference was on average 3.1–3.2 °C in April and May (Figure 6). At the end of spring in June, the difference was 2.2–4.1 °C in the lines at individual depths. During the spring season, the temperature rises on average by 5.2 °C at the 0.10 m level. The temperature increase at the deeper levels is less, i.e., 1.5–2.7 °C. At the deepest level (1.00 m), at the beginning of the period, the temperature increased by 1.3 °C. By the turn of May to June, all temperatures increased by 2.2–2.5 °C, depending on the distance from the building. The temperature difference between the extreme depth levels (0.10 m and 1.00 m) for the whole spring period was 3.5–10.3 °C.

3.5. Soil Temperature in Measurement Lines and Levels

The detailed analysis of temperatures in soil allowed determination of the impact of the building on the temperature in the surrounding soil (Figure 7). The temperatures gradually dropped in November and December. The temperature difference between the extreme depth levels was 3.1–4.4 °C in November and 4.1–5.2 °C in December. During the winter period, the soil temperature dropped further by 0.2–0.4 °C in lines I–N located farthest from the building foundation. However, in lines nearest to the foundation (i.e., E–H) the soil temperature increased by 0.2–1.0 °C on average. During the spring, the soil temperature increased by 2.2–2.5 °C, depending on the distance from the building. No significant impact of the building on the thermal conditions in surrounding soil was determined during the summer period.

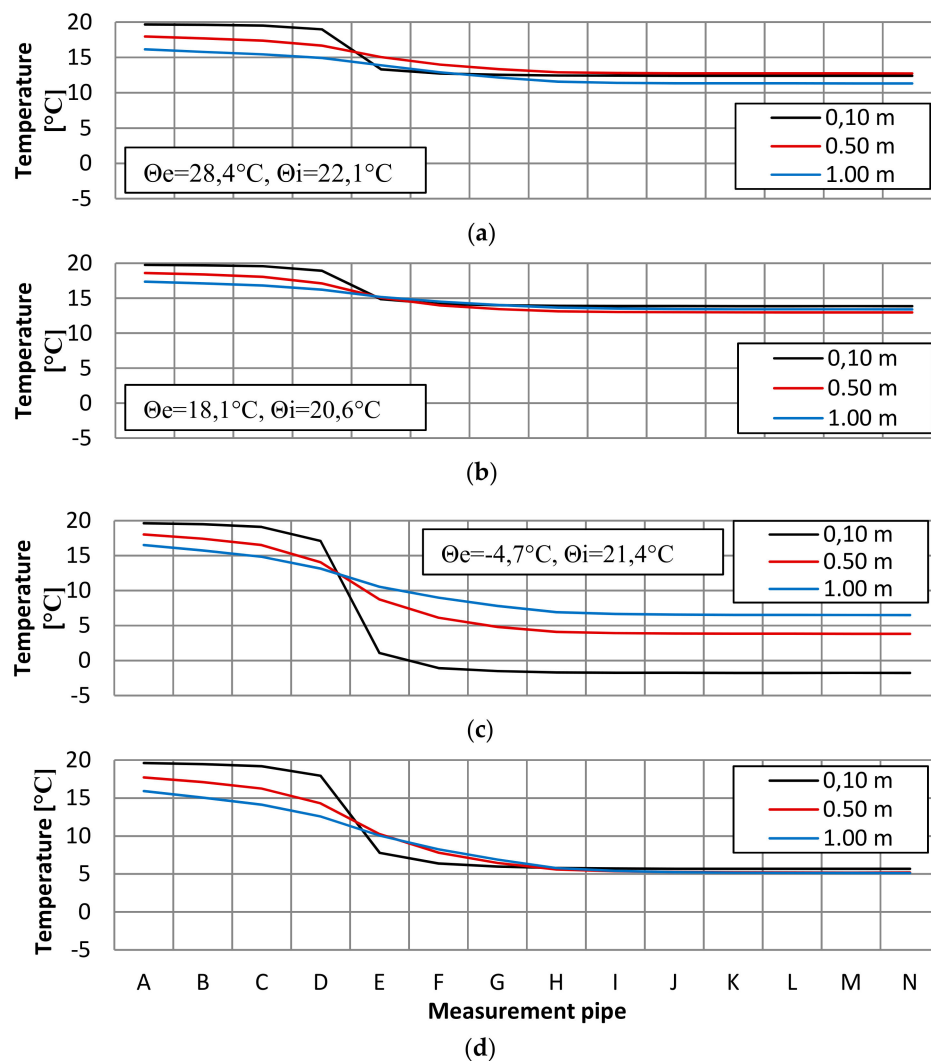


Figure 7. Soil temperature in measurement lines and levels and interior (Θ_i) and exterior (Θ_e) air temperature: (a) summer (15 July), (b) autumn (15 October), (c) winter (15 January), and (d) spring (15 April).

Figure 8 presents soil temperature boxplots for selected measurement points. Statistically significant differences ($\alpha = 0.05$) were determined for points E–I. At the longer distance (above 3.30 m), the temperature differences between the lines (J–N) were not statistically significant. At the end of the winter period, the difference between the average temperature at the 0.10 m level and at the 1.00 m level was 0.6°C . The difference between the lines E and N was 4.8°C . The range of building impact on the surrounding soil was significantly less in the spring period. The difference between the average temperature at the 0.10 m level and at the 1.00 m level was 7.2°C . The difference between the lines E and N was 4.0°C , but the statistically significant differences were recorded up to a distance of about 2.0 m from the building (line H).

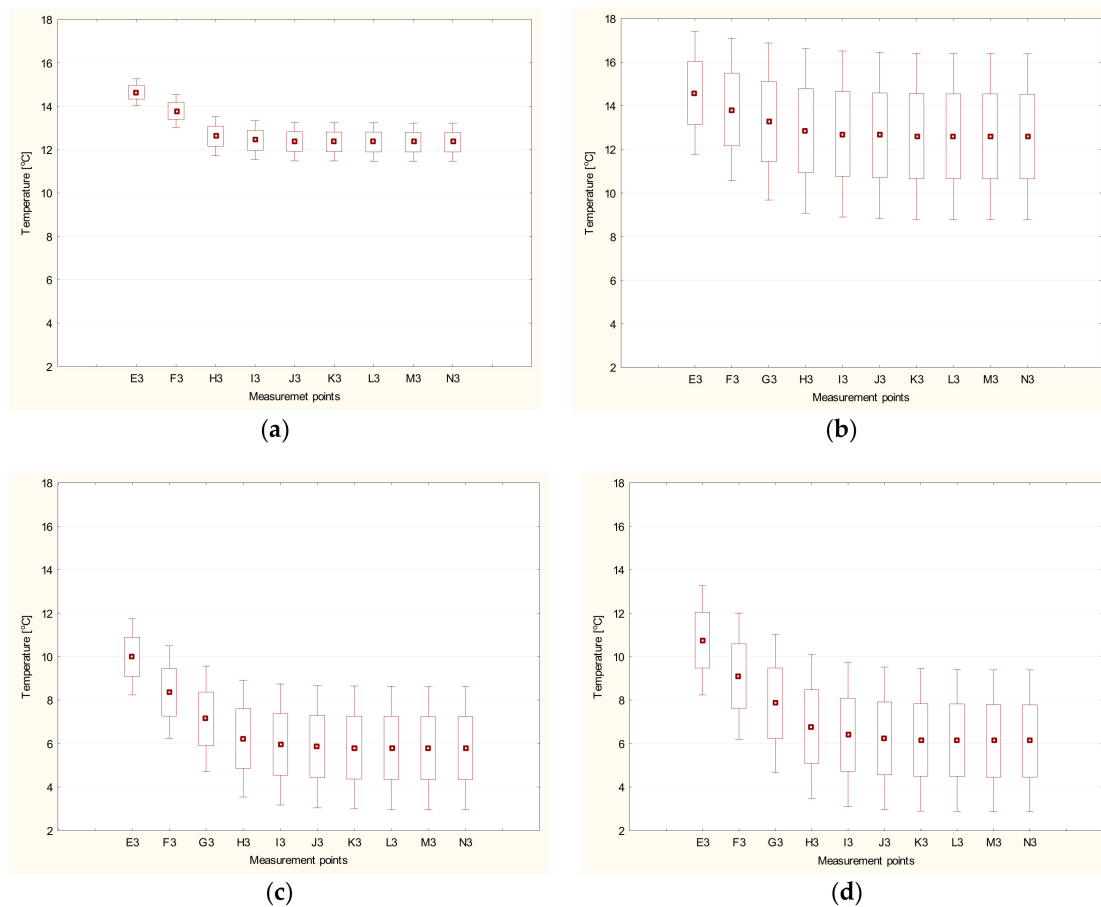


Figure 8. Soil temperatures in selected measurement points located in the soil surrounding the building at a depth of 1.00 m in (a) summer, (b) autumn, (c) winter, and (d) spring.

3.6. Heat Exchange with the Ground

The analysis of heat exchange between the building and the soil indicates that the thermal energy gains from the soil under the floor and in the immediate surroundings of the building occurred only in the summer period when the central heating was inactive. The soil heated during the day and gave up heat at night. The total heat gains from the soil during the summer were 16 kWh (0.15 kWh/m²) (Figure 9). During the autumn, winter, and spring periods the soil received the heat. The greatest energy losses from the building to the soil were 2082 kWh (21.24 kWh/m²), which were recorded during the winter period. During spring, the heat losses to the soil dropped by 38% as compared to winter and were 1294 kWh (13.20 kWh/m²). The heat exchange with soil in autumn was similar to that in spring. The heat losses to the soil were lower by 150 kWh (1.53 kWh/m²) than in spring.

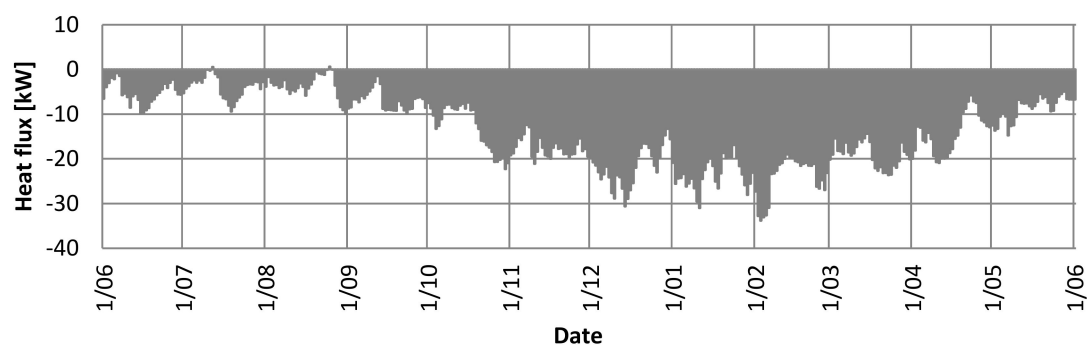


Figure 9. Building–soil heat exchange by seasons.

The thermal distribution of isolines under and in the surroundings of the building and the heat stream flow directions for four periods are presented in Figure 10.

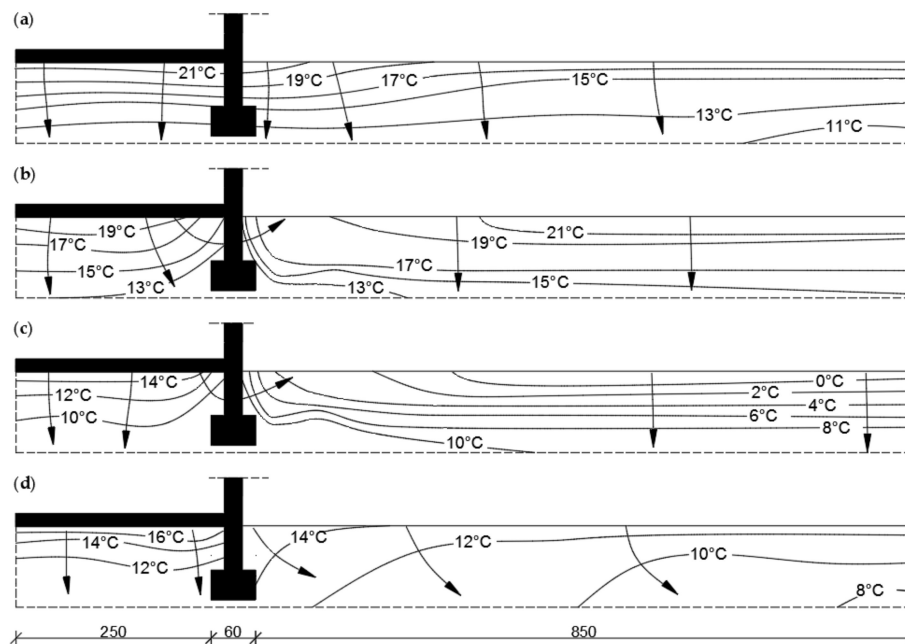


Figure 10. Soil temperature under and in the surroundings of the building and heat stream flow directions in (a) summer, (b) autumn, (c) winter, and (d) spring.

During the summer, the top surface of soil surrounding the building (E1–N1) reached temperatures from 17 °C to 21 °C, and the heat flow directions were from the building to the ground. The thermal range of building interaction with the soil was 3.3 m from the foundation and at the end of autumn it was 1.8 m–2.0 m. The thermal distribution of isolines under and in the surroundings of the building during winter shows that the warmest soil area was the lowest level, 1.00 m closest to the foundation, and the heat flow directions are towards the surface and towards the building. The thermal range of building interaction with the soil during the entire winter was between 2.20 m and 2.40 m from the foundation. The heat flow direction reverses at the turn of April and May. The thermal distribution of isolines in the surroundings of the building indicates that the warmest soil area was the uppermost level 0.10 m closest to the foundation. The soil temperature just below the surface was 12.0–14.0 °C that at the 1.00 m level. The lowest temperature was 9.0 m away from the building at the depth of 1.00 m. The heat flow directions are downwards and towards the building fencing. The thermal range of building interaction with soil was 1.60 m from the foundation at the beginning of the period and it decreased to 1.20 m by the end of spring.

4. Discussion

During the autumn and winter, when the temperature difference between the soil zones near the building and farthest from the building was the greatest, the heat exchange between these zones was intensive. The heat stream flow direction during autumn and winter in the zone outside the building was upwards, from the deeper layers to the air. The situation was the opposite during the summer, i.e., the soil from deeper layers received heat from higher layers.

The heat stream flow directions during the autumn and winter indicate the need for a reduction of heat flow from the building to the outdoor zone which should make the energy management more rational and improve the building comfort and use. During the summer, the building may be a heat receiver because its temperature is much lower than the ambient temperature [31]. The studies conducted in the last decade have generally focused on the soil temperature in the closest surroundings

of buildings, mainly in the vertical cross section [32,33]. The range of the building's impact on soil can affect the energy management of neighboring buildings. This can lead to the accumulation of heat outflow from the building which in favorable spatial conditions could be used, for example, to feed the lower heat pump source and increase its energy efficiency [25]. The results obtained from the field tests can be used to validate the calculation models and facilitate the design of devices that are based on the energy accumulated in soil [30,33]. The knowledge of the thermal impact of a building and other technical infrastructure items related to the temperature distribution in soil will allow a correct management of intensively built-up areas.

5. Conclusions

This study indicates that the role of soil in the energy management of a residential building varies during the year. The soil temperatures depend on the outdoor air temperature and the indoor air temperature. The surface soil layer is the most sensitive to changes of the outdoor air temperature. The amplitude of soil temperature fluctuations during the period of study varied depending on the measurement point and was in the 0.6–22.6 °C range. The highest temperature during the entire period of study (22.6 °C) was in line A at a depth of 0.10 m closest to the foundation of the heated building. The lowest temperature (0.6 °C) was recorded at a depth of 0.10 m in line F, 9.0 m away from the building. During winter and spring, the soil surrounding the building is a heat receiver, whereas, during autumn the soil gives up the heat accumulated during warm summer days. The largest share of soil in the heat exchange is during winter and is 38% higher than during spring and autumn. The range of the building's thermal impact on the soil varied from 2.00 m to 3.30 m and depended on the season and depth. The greatest range of the building's thermal impact was recorded in autumn, 3.30 m away from the building. The least range was recorded at the end of the spring period, 2.00 m away from the building foundation.

The obtained test results are not universal, as they concern only the case study. As mentioned above, the conducted tests will be used to validate the calculation model, based, for example, on the numerical method of elementary balances, which can be used for various boundary conditions. As a result, it will be possible to use the research developed in a universal manner for different climate zones.

Author Contributions: Conceptualization, G.N.; Data curation, G.N.; Formal analysis, G.N. and P.S.; Methodology, G.N.; Software, P.S.; Supervision, G.N.; Visualization, P.S.; Writing—original draft, G.N. and P.S.; Writing—review&editing, G.N. and P.S.

Funding: This research received no external funding.

Conflicts of Interest: The authors declare no conflicts of interest.

References

1. Mengjie, S.; Ning, M.; Yingjie, X.; Shiming, D. Challenges in, and the development of, building energy saving techniques, illustrated with the example of an air source heat pump. *Ther. Sci. Eng. Prog.* **2019**, *10*, 337–356.
2. Sher, F.; Kawai, A.; Gulec, F.; Sadiq, H. Sustainable energy saving alternatives in small buildings. *Sustain. Energy Technol. Assess.* **2019**, *32*, 92–99.
3. Ruiz, M.C.; Romero, E. Energy saving in the conventional design of a Spanish house using thermal simulation. *Energy Build.* **2011**, *43*, 3226–3235. [[CrossRef](#)]
4. Herbut, P.; Rzepczyński, M.; Angrecka, S. Analysis of the efficiency and investment profitability of a solar water heating system in a multi-family building. *J. Ecol. Eng.* **2018**, *19*, 75–80. [[CrossRef](#)]
5. Nawalany, G.; Sokołowski, P. Analysis of hygrothermal conditions of external partitions in an underground fruit store. *J. Ecol. Eng.* **2016**, *17*, 75–82. [[CrossRef](#)]
6. Nawalany, G.; Sokołowski, P.; Herbut, P.; Angrecka, S. Development of selected parameters of microclimate in a stand alone cellar plunged into soil. *J. Ecol. Eng.* **2017**, *18*, 156–161. [[CrossRef](#)]
7. Popiel, C.O.; Wojtkowiak, J.; Biernacka, B. Measurements of temperature distribution in ground. *Exp. Ther. Fluid Sci.* **2001**, *25*, 301–309. [[CrossRef](#)]

8. Tinti, F.; Barbaresi, A.; Benni, A.; Torreggiani, D.; Bruno, R.; Tassinari, P. Experimental analysis of shallow underground temperature for the assessment of energy efficiency potential of underground wine cellars. *Energy Build.* **2014**, *80*, 451–460. [[CrossRef](#)]
9. Sartori, I.; Hestnes, A.G. Energy use in the life cycle of conventional and low-energy buildings: A review article. *Energy Build.* **2007**, *39*, 249–257. [[CrossRef](#)]
10. Baggs, S.A. Remote prediction of ground temperature in Australian soils and mapping its distribution. *Solar Energy* **1983**, *30*, 351–366. [[CrossRef](#)]
11. Chow, T.T.; Long, H.; Mok, H.Y.; Li, K.W. Estimation of soil temperature profile in Hong Kong from climatic variables. *Energy Build.* **2011**, *43*, 3568–3575. [[CrossRef](#)]
12. Mihalakakou, G.; Santamouris, M.; Asimakopoulos, D.; Argiriou, A. On the ground temperature below buildings. *Solar Energy* **1995**, *55*, 355–362. [[CrossRef](#)]
13. Radoń, J.; Bieda, W.; Lendelova, J.; Pogran, S. Computational model of heat exchange between dairy cow and bedding. *Comput. Electron. Agric.* **2014**, *107*, 29–37. [[CrossRef](#)]
14. Nawalany, G.; Bieda, W.; Radoń, J.; Herbut, P. Experimental study on development of thermal conditions in ground beneath a greenhouses. *Energy Build.* **2014**, *69*, 103–111. [[CrossRef](#)]
15. Nawalany, G.; Radoń, J.; Bieda, W.; Sokołowski, P. Influence of selected factors on heat exchange with the ground in a greenhouse. *Trans. ASABE* **2017**, *60*, 479–487.
16. Staniec, M. Analiza wpływu częściowego zagłębienia budynku w gruncie na jego bilans energetyczny. In *Rozprawa Doktorska*; Politechnika Wrocławska: Wrocław, Polska, 2009.
17. Martin, S.; Canas, I. A comparison between underground wine Cellary and aboveground storage for the aging of Spanish wines. *Trans. ASABE* **2006**, *49*, 1471–1478. [[CrossRef](#)]
18. Janssen, H. The Influence of Soil Moisture Transfer on Building Heat Loss via the Ground. Ph.D. Thesis, Departement Burgerlijke Bouwkunde, Katholieke Universiteit Leuven, Leuven, Belgium, 2002.
19. Deru, M. Ground-Coupled Heat and Moisture Transfer from Buildings. Ph.D. Thesis, Colorado State Univeristy, Fort Collins, CO, USA, 2001.
20. Popiel, C.O.; Wojtkowiak, J. Temperature distributions of Grodnu in the Urban region of Poznan City. *Exper. Ther. Fluid Sci.* **2013**, *51*, 135–148. [[CrossRef](#)]
21. Larwa, B.; Kupiec, K. Study of temperature distribution in the ground. *Chem. Process Eng.* **2019**, *40*, 123–137.
22. Staszczuk, A.; Kuczyński, T.; Wojciech, M.; Ziembicki, P. Comparative calculation of heat exchange with the ground in residential building including periods of heat waves. *Civil Environ. Eng.* **2016**, *21*, 109–119.
23. Erol, S.; Francois, B. Multilayer analytical model for vertical ground heat exchanger with groundwater flow. *Geothermics*. **2018**, *71*, 294–305. [[CrossRef](#)]
24. Zhao, B. Study on heat transfer of ground heat exchanger based on wedgelet finite element method. *Int. Commun. Heat Mass Trans.* **2016**, *74*, 63–68. [[CrossRef](#)]
25. Kupiec, K.; Larwa, B.; Gwadera, M. Heat transfer in horizontal ground heat exchangers. *Appl. Ther. Eng.* **2015**, *75*, 270–276. [[CrossRef](#)]
26. Fidorów, N.; Szulgowska-Zgrzywa, M. The influence of the ground caupled heat pump's labor on the ground temperature in the boreholes—Study based on experimental data. *Appl. Ther. Eng.* **2015**, *82*, 237–245. [[CrossRef](#)]
27. Flaga-Maranczyk, A.; Schnotale, J.; Radoń, J.; Wąs, K. Experimental measurements and CFD simulation of a ground source heat exchanger operating at a cold climate for a passive house ventilation system. *Energy Build.* **2014**, *68*, 562–570. [[CrossRef](#)]
28. Bertram, E. Solar Assisted Heat Pump Systems with Ground Heat Exchanger - Simulation Studies. *Energy Procedia*. **2014**, *48*, 505–514. [[CrossRef](#)]
29. Larwa, B. Heat transfer model to predict temperature distribution in the ground. *Energies* **2019**, *12*. [[CrossRef](#)]
30. Hassanzadeh, R. Replacing the wet cooling tower with a ground source heat exchanger as a clean technology. *J. Build. Eng.* **2018**, *18*, 331–342. [[CrossRef](#)]
31. Giraldo, M.A.; Bosch, D.; Madden, M.; Usery, L.; Finn, M. Ground and surface temperature variability for remote sensing of soil moisture in a heterogeneous landscape. *J. Hydrol.* **2009**, *368*, 214–223. [[CrossRef](#)]

32. Beier, R.A.; Acuna, J.; Mogensen, P.; Palm, B. Vertical temperature profiles and borehole resistance in a U-Tube borehole heat exchanger. *Geothermics* **2012**, *44*, 23–32. [[CrossRef](#)]
33. Beng, K.; Noguchi, M. Verification of the performance of a vertical ground heat exchanger applied to a test house in Melbourne, Australia. *Energies* **2017**, *10*. [[CrossRef](#)]



© 2019 by the authors. Licensee MDPI, Basel, Switzerland. This article is an open access article distributed under the terms and conditions of the Creative Commons Attribution (CC BY) license (<http://creativecommons.org/licenses/by/4.0/>).